research articles Journal of proteome research

Proteomic Profiling of Erythrocyte Proteins by Proteolytic Digestion Chip and Identification Using Two-Dimensional Electrospray Ionization Tandem Mass Spectrometry

Yu-Chang Tyan,*,† Shiang-Bin Jong,‡ Jiunn-Der Liao,§ Pao-Chi Liao,† Ming-Hui Yang,|| Chia-Yuan Liu,† Ruth Klauser,# Michael Himmelhaus,⊥ and Michael Grunze⊥

Department of Environmental & Occupational Health, National Cheng Kung University, No.1, Ta−Hsueh Road, Tainan 701, Taiwan, Republic of China, Department of Nuclear Medicine, Kaohsiung Medical University, 100 Shi-Chuan first Road, Kaohsiung 807, Taiwan, Republic of China, Department of Materials Science and Engineering, National Cheng Kung University, No.1, Ta−Hsueh Road, Tainan 701, Taiwan, Republic of China, Department of Chemistry, Texas Christian University, 2800 S. University Drive, Fort Worth, Texas 76129, United States of America, National Synchrotron Radiation Research Center, 101 Hsin-Ann Road, Hsinchu Science Park, Hsinchu 300, Taiwan, Republic of China, and Lehrstuhl für Angewandte Physikalische Chemie, Universität Heidelberg, Im Neuenheimer Feld 253, 69120 Heidelberg, Germany

Received November 30, 2004

Self-assembled monolayers (SAMs) on coinage metal provide versatile modeling systems for studies of interfacial electron transfer, biological interactions, molecular recognition, and other interfacial phenomena. The bonding of enzyme to SAMs of alkanethiols onto gold surfaces is exploited to produce an enzyme chip. In this work, the attachment of trypsin to a SAMs surface of 11-mercaptoundecanoic acid was achieved using water soluble *N*-ethyl-*N*′-(3-dimethylaminopropyl) carbodiimide hydrochloride and *N*-hydroxysuccinimide as coupling agent. A two-dimensional liquid-phase separation scheme coupled with mass spectrometry is presented for proteomic analysis of erythrocyte proteins. The application of proteomics, particularly with reference to analysis of proteins, will be described. Surface analyses have revealed that the X-ray Photoelectron Spectroscopy (XPS) C1s and N1s core levels illustrate the immobilization of trypsin. These data are also in good agreement with Fourier Transformed Infrared Reflection-Attenuated Total Reflection (FTIR-ATR) spectra for the peaks at Amide I and Amide II. Using two-dimensional nano-high performance liquid chromatography electrospray ionization tandem mass spectrometry (2D nano-HPLC−ESI−MS/MS) system observations, analytical results have demonstrated the erythrocyte proteins digestion of the immobilized trypsin on the functionalized SAMs surface. For such surfaces, it also shows the enzyme digestion ability of the immobilized trypsin. The experiment results revealed the identification of 272 proteins from erythrocyte protein sample. The terminal groups of the SAMs structure can be further functionalized with biomolecules or antibodies to develop surface-base diagnostics, biosensors, or biomaterials.

Keywords: proteomics • two-dimensional nano-high performance liquid chromatography electrospray ionization tandem mass spectrometry (2D nano-HPLC−ESI−MS/MS) • protein digestion • self-assembled monolayers (SAMs)

Introduction

Proteomics characterization of protein for identification of disease-specific biomarkers provides a powerful tool to gain deep insights into disease mechanisms in which proteins play a major role. It can also investigate structures and functions of protein complexes working as molecular micro-machines expressed spatiotemporally through protein−protein interactions and signal transduction by post-translational modification.[1] Protein profiling has often been performed by the "classical" one- or two-dimensional sodium dodecyl sulfate polyacryamide gel electrophoresis (1D- or 2D-PAGE) based on the densitometric quantification of proteins visualized using dyes on gel. After in-gel enzymatic digestion of the subject protein sports, the resulting peptides are subjected to matrix-assisted laser desorption ionization (MALDI) or electrospray ionization (ESI) mass spectrometry. However, 2D-PAGE has some fundamental problems and limitations. The technique is laborious and time-consuming.[2] In clinical and diagnostic proteomics, it is essential to develop a comprehensive and

* To whom correspondence should be addressed. E-mail: yctyan@mail.ncku.edu.tw. Fax: 886 6 3137999.
† Department of Environmental & Occupational Health, National Cheng Kung University.
‡ Kaohsiung Medical University.
§ Department of Materials Science and Engineering, National Cheng Kung University.
|| Texas Christian University.
National Synchrotron Radiation Research Center.
⊥ Universität Heidelberg.

10.1021/pr0497780 CCC: $30.25
Published on Web 04/21/2005

robust system for proteome analysis.[3] Recent advances in liquid chromatography, mass spectrometers, and data analysis software enable the direct analysis of extremely complex peptide mixtures, often referred to as shotgun proteomics or multidimensional protein identification technology (MudPIT).[4] Although multidimensional liquid chromatography/tandem mass spectrometry (MD−LC/MS/MS) systems have been recently developed as powerful tools especially for identification of protein complexes, these systems still some drawbacks in their application to clinical research that requires an analysis of a large number of protein samples.[2]

Therefore, we have constructed a technically simple and high throughput protein profiling system comprising two-dimensional nano-high performance liquid chromatography and electrospray ionization tandem mass spectrometry (2D nano-HPLC−ESI−MS/MS). This system integrates a strong cation exchange (SCX) chromatography and a nano-LC/MS/MS system with nano-flowing reversed-phase chromatography. 2D nano-HPLC−ESI−MS/MS spectrometry is a highly sensitive and selective analytical technique that has become a powerful method for the identification of proteins present in complex mixtures. A driving forces in proteomics is the discovery of biomarkers, proteins that change in concentration or state in associations with a specific biological process or disease.

Self-assembled monolayers (SAMs) have received a great deal of attention for their fascinating potential technical applications such as nonlinear optics and device patterning.[5−7] They were also used as an ideal model to investigate the effect of intermolecular interactions in the molecular assembly system.[8,9] It was very convenient to introduce functional structure as tail group on SAMs, and to investigate different molecular interactions with tail group on SAMs as induced by particular species.[10,11]

SAMs form spontaneously by chemisorptions and self-organization of thiolate organic molecules onto a surface of appropriate substrate. SAMs were usually prepared by immersing a substrate into a solution containing a ligand that was reactive to the surface or by exposing the substrate to the vapor of the reactive species.

The most characterized system of SAMs was preferably the alkanethiolates (AT) on gold (Au), rather than other metals such as platinum, copper, or silver, because Au did not have a stable oxide. SAMs formed by adsorption of either alkanethiols onto Au or alkylsilanes onto hydroxylated surfaces constitute an important class of model surfaces for fundamental studies of protein or enzyme adsorption. The process was assumed to occur with the loss of hydrogen, by the immersion of Au substrate in a dilute solution of the AT and the formation of well-ordered SAMs on Au surface.[12−15] The AT SAMs not only provide excellent model system to study fundamental aspects of surface properties such as wetting[16] and tribology,[17] but also were promising candidates for potential applications in the fields of biosensors,[18] biomimetics,[19] and corrosion inhibition.[20] Recently, the bonding of enzymes to SAMs of AT on Au surfaces has begun to receive attention as a method of constructing enzyme electrodes.

In this study, we practice two kinds of the AT SAMs, include: 1-Dodecanethiol and 11-mercaptoundecanoic acid to prepare the SAMs on the Au (111) surface, followed by the coupling of a biological sensing element such as an enzyme, protein, cell or antibody with a transducer, either chemical, electrochemical, optical, or piezoelectric, which was regarded as the basis to integrate an enzyme chip. For example, water-soluble *N*-ethyl-*N*′-(3-dimethylaminopropyl) carbodiimide hydrochloride (EDC) and *N*-Hydroxysuccinimide (NHS) were utilized to activate the tail group of O═C−OH[21−23] and then immersed in the trypsin-contained solution to bind with $-NH_2$ in trypsin.

As shown in the literatures,[24−26] a variety of analytical techniques such as X-ray Photoelectron Spectroscopy (XPS), Infrared Reflection Absorption Spectroscopy (IR−RAS), Fourier Transformed Infrared with Attenuated Total Reflection (FTIR−ATR), Elliposometer and Contact angle measurements, the AT SAMs were densely packed films. The general understanding was that the molecules were attached to the surface via an Au-thiolate bond, though some results have indicated the possible formation of disulfides. Elliposometer identified the molecular confirmations of alkyl chains in the completed monolayers. The molecular structure and organization of the SAMs were investigated using surface-sensitive techniques such as FTIR−ATR and XPS. A 2D nano-HPLC−ESI−MS/MS was used to obtain the proteins identification of tryptic peptides in this study.

In this experiment, it tends to complete a preliminary study for a potential biomedical application of functionalized SAMs to immobilize with enzyme as a protein mixture digestion biochip. A mass spectrometry system could use the biochip for a protein mixture digestion and identification. We present proteomic-profiling data of erythrocyte proteins identification using 2D nano-HPLC−ESI−MS/MS. This type of surface can also be successfully used to develop a feasible procedure of producing surface-base enzyme biochip. Of the combined with proteomics approaches, it can be used for biomarker discovery in the future.

Materials and Methods

Formation of SAMs. Au was the most frequently used coinage metal, as it does not have a stable oxide under ambient conditions. A 200 nm thick Au film was prepared by electron beam evaporation onto Si (111) surface (*Silicon Sense*) primed with an adhesion layer of 20 nm Ti. Prior to each experiment, all containers, equipment and supplies were carefully cleaned by first rinsing with absolute ethanol, then with 30% hydrogen peroxide, again with absolute ethanol, and finally with the pure solvent to be used in the adsorption experiments. The Au (111) substrates with a standard dimension of 1.5 × 1.5 cm were cleaned by 30% hydrogen peroxide solution for 15 s. followed rinsing by high-purity ethanol (RDH 32205, Riedel-deHaën), and then immersed into 0.5 mM ethanolic alkanethiol solution at room temperature for 12 h.[26] The alkanethiols adsorb spontaneously from solution onto the Au surface. Two kinds of chemicals for SAMs preparation were used: 1-Dodecanethiol: $C_{12}H_{26}S$ (44130, Fluka), and 11-mercaptoundecanoic acid: $C_{11}H_{22}O_2S$ (450561, Aldrich). The reference surface for IR−RAS: $C_{20}D_{42}S$ was also utilized. The functionalized thiol groups were chemisorbed onto Au surface via the formation of thiolate bonds.[27]

Immobilization of Trypsin onto SAMs. To immobilize trypsin, the 11-mercaptoundecanoic acid/Au surface was immersed in the coupling agent: 75mM *N*-ethyl-*N*′-(3-dimethylaminopropyl) carbodiimide hydrochloride (EDC, E−6383, Sigma) and 15mM *N*-hydroxysuccinimide (NHS, H-7377, Sigma) at 4 °C for 30 min.[28,29] Water-soluble EDC and NHS were used for activating O═C−OH[22,23] and then the EDC−NHS buffer was removed and replaced by the 0.2 μg/μL (w/v) trypsin digestion buffer (V511A, Promega) at 4 °C for 24 h. The SAMs wafer was thereafter washed by DI water and dried out mildly at 4 °C.

The preparation was carried out in a clean environment. During the reactions, EDC was capable to convert the carboxylic acids into a reactive intermediate, which was susceptible to be attacked by amine group. In some cases, both of EDC and NHS were used as they produce a more stable reactive intermediary, which has been shown to give a greater reaction yield.[18]

The amounts of immobilized trypsin on SAMs surface was measured by an estimation of[30,31]

$$\text{Immobilized trypsin } (\mu g/cm^2) = (Wt - W)/A$$

where A was the dimensional area of the SAMs surface, W and Wt were the weights of SAMs surface before and after trypsin immobile process.

Ellipsometric Measurement. The thickness of the SAMs monolayers was determined by an optical ellipsometer (LPS-400, J. A. Woollam Co., Inc.), equipped with a He/Ne laser of λ = 632.8 nm as the light source. The light has an incident angle of 70°, relative to the surface normal. After monolayer formation, each sample was analyzed, and the film thickness was calculated from three-phase parallel layer model: ambient, organic film, and Au substrate models. Using the average complex refractive index of the individual sample and a real refractive index of 1.45 for the film. The value of 1.45 was representative for the adsorbate precursors, which facilitated a comparison with the thickness that has been reported for a variety of monolayers elsewhere.[25,32]

Contact Angle Measurement. The contact angles (θ) were measured in air using a goniometer (Krüss apparatus). A Milli-Q grade water (Millipore Co., Inc.) was used to contact with the sampling dimension by the sessile drop method. For this measurement, a 2 μL droplet was placed slightly on the specimen with the needle of a syringe. The value of θ was determined as the volume of the droplet was slowly increased.[25,32]

X-ray Photoelectron Spectroscopy Measurement. XPS spectra were acquired with a Physical Electronics PHI 1600 ESCA photoelectron spectrometer with a magnesium anode at 400 W and 15 kV−27 mA (Mg K_α 1253.6 eV, type 10−360 spherical capacitor analyzer). The specimens were analyzed at an electron takeoff angle of 70°, measured with respect to the surface plane. The operating conditions were as follows: pass energy 23.4 eV, base pressure in the chamber below 2×10^{-8} Pa, step size 0.05, total scan number 20, scan range 10 eV (for multiplex scan). The peaks were quantified from high-resolution spectra, obtained by using a monochromatic Mg X-ray source. Elemental compositions at the surface using C1s, O1s and N1s core level spectra were measured and calculated from XPS peak area with correction algorithms for atomic sensitivity. The XPS spectra were fitted using Voigt peak profiles and a Shirley background.

Fourier Transformed Infrared Reflection−Absorption and Attenuated Total Reflection Spectrosocopies. All infrared (IR) spectroscopy optical benches were acquired with a conventional Fourier transformed (FT) Spectrometer (FTS-175C, Bio-Rad) equipped with a KBr beam splitter and a high-temperature ceramic source. Win-IR, Win-IR Pro (Bio-Rad), and Origin 6.0 (Microcal Software, Inc.) were used for the data acquisition and analysis. The IR spectra were obtained using p-polarized beam incident at a grazing angle of around 80° with respect to the surface normal. The spectra were measured by a liquid-nitrogen cooled, narrow band MCT detector. The spectra were recorded with a resolution of 4 cm^{-1} using about 500 scans and an optical modulation of 15 kHz filter. Alternatively, the analytical instruments for identifying chemical structures (Amide I and Amide II) was confirmed by FTIR spectrometry, using a Jasco-410 FTIR spectrometer fitted with an Attenuated Total Reflection (ATR, Pike Instrument) device containing a germanium crystal and Harrick KBr prism with 200 scans and spatial resolution of 2 cm^{-1}.

Erythrocytes Proteins Preparation. Venous blood was obtained from six normal young individuals, ages in the ranging of 20−25, who had not consumed aspirin or other nonsteroidal antiinflammatory drugs for at least two weeks; the blood was collected in a glass vacutainer (5 mL) and mixed with the anticoagulant 3.8% (w/v) sodium citrate (9 vol. blood: 1 vol. citrate) in tubes. Fresh blood of 10 mL from each donor was sampled. Erythrocytes were prepared by centrifugation of whole blood at 300 × g for 10 min. at 4 °C. The upper part of human plasma and buffy coat (white blood cells with a part of platelets) were removed with a micropipet. Erythrocytes were washed twice by HEPES buffered saline (83264, Fluka). Erythrocyte count of sample suspension in HEPES buffered saline was adjusted to $3.0 \pm 0.1 \times 10^3$ μL^{-1} by a hemacytometer (Hausser Scientific)[33] and then 1 mL sample was frozen at −20 °C. Erythrocytes were broken by ultrasonic cell disrupter (Sonics VCX-750, Sonics & materials, Inc.) and centrifuged at 15 000 × g for 20 min. at 4 °C. The protein suspension was obtained with a micropipet. The protein concentration of the erythrocytes samples were measured by Bradford method[34] and adjusted to 1 mg/mL by 25 mM ammonium bicarbonate.

In the 2D nano-HPLC−ESI−MS/MS analysis of erythrocyte proteins, 20 μL of the protein suspension sample described above was deposited on the trypsin-immobilization surface. The samples were allowed to shake slowly at 37 °C, 30 min using an incubator for digestion and then transferred into vials.

Protein Identification by 2D nano-HPLC−ESI−MS/MS. 2D nano-HPLC−ESI−MS/MS was performed to identify erythrocyte proteins. The protein tryptic digests were fractionated using a flow rate of 200 nL/min with a nano-HPLC system (LC Packings, Netherlands) coupled to an ion trap mass spectrometer (LCQ DECA XP Plus, ThermoFinnigan, San Jose, CA) equipped with an electrospray ionization source. The HPLC system consists of three units: a micropump/UV detection module (UltiMate), a column switching module (Switchos), and a micro autosampler module (Famos). The protein have been digested by trypsin chip and resulting peptides were separated using a strong cation-exchange column (BioX-SCX column: 500 μm I. D. × 15 mm; 2-D Capillary LC Kit, P/N 161579, LC Packings, Netherlands) in the first dimension and a reverse phase (RP) nano separation column (C18 PepMap trapping column: 300 μm I. D. × 5 mm) in the second dimension. A sample (10 μL) contain of 10 μg tryptic peptide was loaded into the BioX-SCX column. Using column-switching technique, with a Switchos module, peptides were loaded onto the Bio-SCX column and preconcentrated on the C18 PepMap nano RP trapping column. The loading flow of Switchos was set to 30 μL/min and the loading solvent was 0.1% formic acid (pH = 3.0). 10 μL of ammonium acetate solution with concentrations of 0, 10, 20, 50, 100, 200, 400, 600, 800, 1000, and 2000 mM have been injected to elute peptides from the BioX-SCX column[35]. The BioX-SCX column was switched off-line and the excess of salt washed from the RP trap column. The RP separation and chromatographic elution were performed using a 200 min linear acetonitrile solvent gradient from 100% buffer A (5% acetonitrile/0.1% formic acid) to 60% buffer B (80%

Table 1. Ellipsometric Thickness and Water Contact Angles Measurement of the SAMs on Au (111)

monolayer compound		thickness (Å)	contact angle (deg)
$SD-(CD_2)_{19}-CD_3$	(for IR reference)	25.68 ± 0.60	105.17 ± 0.42
$SH-(CH_2)_{11}-CH_3$	1-Dodecanethiol	14.42 ± 0.55	97.00 ± 0.29
$SH-(CH_2)_{10}-COOH$	11-mercaptoundecanoic acid	16.57 ± 0.55	14.67 ± 0.46

acetonitrile/0.1% formic acid). The peptide separation was performed on a C18 microcapillary column (75 μm I. D. × 15 cm) using the UltiMate capillary and nano-separation system. As peptides eluted from the microcapillary column, they were electrosprayed into the ESI−MS/MS with the application of a distal 1.3 kV spraying voltage. Each cycle of one full scan mass spectrum (m/z 450−2000) was followed by three data dependent tandem mass spectra. This entire LC−MS system can be controlled through ThermoFinnigan's Xcalibur software with LC Packings plug-in.

SEQUEST Database Searching. Tandem mass spectrometry data was analyzed by the database search software SEQUEST (Bioworks 3.1, TheroFinnigan, San Jose, CA) to interpret MS/MS spectra. DTA files were generated from product ion scan data (threshold set to 10 000) and used to search against human FASTA protein sequence database (obtained from National Center for Biotechnology Information, NCBI web: ftp.ncbi.bih.gov/blast.db, July 21, 2003). For proteolytic cleavage, only tryptic cleavage was allowed and number of maximal internal (missed) cleavage sites was set to 2. Modifications at cysteine with carboxymethylation and methionine with oxidation were allowed. The mass tolerance of precursor peptide ion was set to 1.4 Da and that for fragment ion tolerance was set to 0, as suggested by the software manufacture. SEQUEST results were filtered with criteria similar to those developed by Yates and co-workers[36]. Briefly, all accepted results had a DelCN (ΔCn) of 0.2 or greater, a value shown to lead to high confidence in a SEQUEST result. The cross-correlation (Xcorr) score is a correlation procedure for the measured and theoretical MS/MS spectra. Xcorr scores of singly charged-peptides had to be higher than 1.9, and those of doubly- and triply charged peptides are higher than 2.2 and 3.75, respectively. When a protein was identified by two or more unique peptides possessing SEQUEST scores that passed the above criteria, no visual assessment of spectra was conducted and the protein was considered present in the sample. Proteins were initially annotated by similarity searches using SWISS-Port/TrEMBL (http://www.expasy.org/) and Bioinformatic Harvester EMBL (http://harvester.embl.de/).

Result and Discussion

Surface Characterization: Film Thickness and Contact Angles. An important metric for the quality of a SAMs surface was given by a direct measurement of the mass coverage of the adsorbate on the surface. Ellipsometry was an invaluable technique for measuring film thickness of alkanethiols adsorbed on SAMs surface, and it was also a useful method to provide key insights into the surfaces of SAMs formed on a variety of metal substrates (e.g., Au, Ag, and Al)[37]. Analytical result from ellipsometry and contact angle measurements of SAMs were summarized in Table 1. The optical ellipsometric characterization obtains a film thickness of 16.57±0.55 Å for 11-mercaptoundecanoic acid/Au, and 14.67 ± 0.46 Å for 1-Dodecanethiol/Au, consistent with the formation of films of one molecular layer. The thickness coincides well with what has been reported previously.[25,26,32] The ellipsometric measurement yields SAMs thickness close to an expected value from space-filling models with a chain-tilt of approximately 30° from the surface normal.

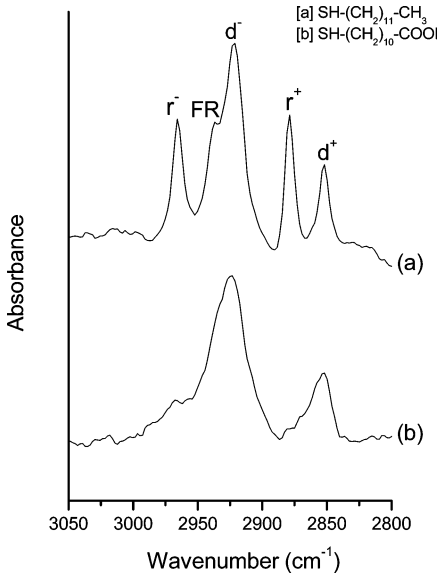

Figure 1. FTIR−RAS spectra show the high-frequency region: 3050−2800 cm^{-1} of the SAMs (a) 1-Dodecanethiol, (b) 11-mercaptoundecanoic acid.

Contact angles for 1-Dodecanethiol/Au surface was indicative of a well-ordered and homogeneous layer with methyl group at the monolayers/ambient interface. Measurement of 11-mercaptoundecanoic acid/Au using water as probe liquid give advancing contact angles of less than 15°, consistent as a high free energy surface. The SAMs surfaces with the carboxyl or the hydroxyl tail group were therefore polarizable and hydrophilic.[38] The contact angles agreed well with Smith et al.,[25] Lestelius et al.[32] and Laibinis et al.[39] The above measurements were found unaffected by extending immersion time in the thiol-containing solutions.

Investigation of Film Structure by FTIR−RAS. All monolayer assemblies were routinely characterized with FTIR−RAS upon preparation. Figure 1 shows that the FTIR−RAS spectra of the SAMs of the alkane and carboxylic acid. The position of the C−H stretching bands of the methylene groups of the alkyl chains indicates the order of the alkyl chains within SAMs. In the spectrum of the SAMs, two absorption bands at 2918 and 2850 cm^{-1} were assigned to asymmetric (d^-) and symmetric (d^+) C−H stretching bands of the methylene groups, respectively.[39] The peak positions of CH_3 stretching modes were consistent with the presence of a dense crystalline-like phase: r^+, 2876 cm^{-1}; FR, 2935 cm^{-1}; r^-, 2963 cm^{-1} in Table 2. These represent in good agreement with Laibinis et al.[39] and Lestelius et al.,[32] who have identified the peaks as the presence of alkene species. The band positions of 11-mercaptoundecanoic acid/Au given in Table 2 indicate that the band frequencies at 1705 and 1400 cm^{-1} were assigned to residual carboxylic acid stretch, ν(C═O) and symmetric carboxylate stretch, $\nu_s(COO^-)$, respectively.[24]

Table 2. Observed Peak Position and Assignments for the Different Monolayers

1-dodecanethiol $SH-(CH_2)_{11}-CH_3$	11-mercaptoundecanoic acid $SH-(CH_2)_{10}-COOH$	assignment [24,32,39]*a*
2963		$\nu_{as}(CH_3)$, r^-
2935		$\nu_s(CH_3)$, FR
2918	2918	$\nu_{as}(CH_2)$, d^-
2876		$\nu_s(CH_3)$, r^+
2849	2850	$\nu_s(CH_2)$, d^+
	1705	$\nu(C{=}O)$
	1400	$\nu_s(COO^-)$

[a] $\nu_{s/as}$: symmetric/asymmetric-stretching modes. FR: Fermi resonance.

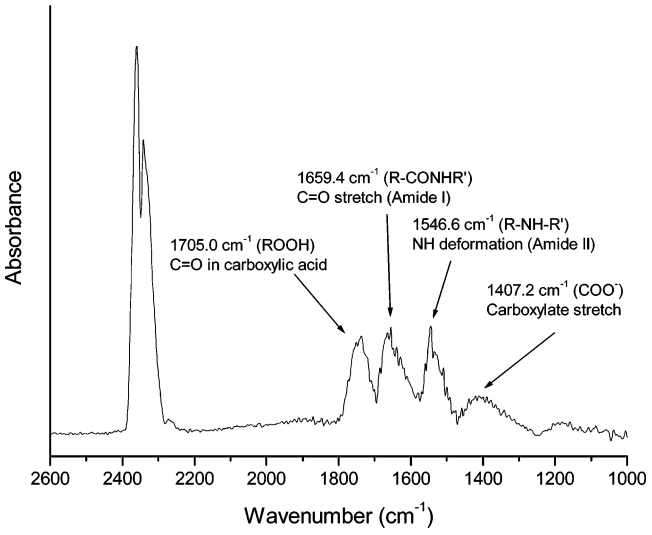

Figure 2. FTIR spectra of the modified SAMs surface: trypsin immobilized on the 11-mercaptoundecanoic acid SAMs surface.

Structural Confirmation of Trypsin-Immobilized Surfaces. In this experiment, water-soluble carbodiimide EDC and NHS were used to convert the carboxylic acid of the11-mercaptoundecanoic monolayer to NHS ester. Reaction of this activated the 11-mercaptoundecanoic-NHS ester monolayer with an aqueous solution of an amine or either ammonia, creates an amide bond with the surface. In this study, water-soluble EDC and NHS were used for activating O═C−OH and immobilizing trypsin. The amounts of immobilized trypsin on SAMs surface was controlled to ca. 0.05 μg/cm^2.

In Figure 2, the peak at 1407.2 cm^{-1} was usually assigned to carboxylate stretch (COO^-). The peak at 1659.4 cm^{-1} was usually assigned to amide I (R−CONHR′, C═O stretching) and the peak at 1546.6 cm^{-1} to amide II (R−NHR′, NH deformation, N−H bending and C−N stretching). These were in good agreement with Ito et al.,[40] Kang et al.[22] and Tyan et al.,[23,41] who have identified the peaks as the presence of O═C−NH species, derived from carboxylic acid and amide structure, where the O═C−OH bond was activated to form O═C−O· by adding water soluble EDC. Thus, the poly-complex between trypsin and 11-mercaptoundecanoic acid was formed; amino groups in trypsin form complexes with carboxyl groups in 11-mercaptoundecanoic acid. Typical chemical compositions of the immobilized trypsin were furthermore characterized using surface sensitive XPS measurement (Figure 3).

Surface analyses used XPS to measure the binding structure on the SAMs metal surface. The binding energy of C1s core level at 289.3 eV (O═C−O) (Figure 3b) and of O1s core level at 532.0 and 533.3 eV examined by XPS, could be assigned to the

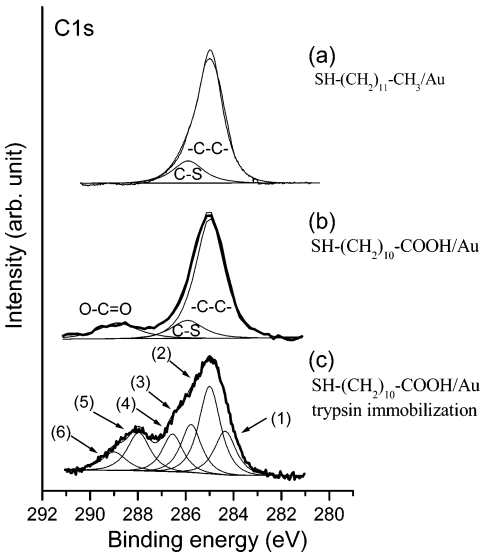

Figure 3. XPS C 1s core level spectra of the modified SAMs surface, (a) 1-Dodecanethiol, (b) 11-mercaptoundecanoic acid, and (c) 11-mercaptoundecanoic acid with trypsin immobilized.

O═C−O structure, which was the characteristic group of 11-mercaptoundecanoic acid.

The XPS C1s core level spectra for the trypsin-immobilized SAMs were shown in Figure 3c. The curves were fitted in accordance with refs 42 and 43. The spectrum was deconvoluted into six peaks: 284.6 and 285.4 eV (hydrocarbon and carbon), 286.3 and 286.5 eV (C with N, amine), 288.1 eV (C with O, carbonyl or amide bond), and 289.3 eV (C with O, carboxylic acid), respectively.[42,43] The trypsin-immobilized SAMs surface displayed a significant increase of C−N and amide group. The groups were corresponding with trypsin molecules (C−N) or a complex between trypsin and 11-mercaptoundecanoic acid (amide group). In Figure 3c, the binding energy at 286.3 and 286.5 eV was assigned to C−N binding in trypsin. The O═C−OH group altered notably owing to the participation of functional group of the 11-mercaptoundecanoic acid binding with trypsin as amide group.

In the XPS measurements, the variations of O1s and N1s with respect to C1s signal ratios were correlated with the significant presence of chemical species at the trypsin-immobilized SAMs surfaces, respectively.

Cellular Location and Known Function of the Identified Proteins. A 2D nano-HPLC−ESI−MS/MS system was used to obtain the fragmentation patterns of tryptic peptides in this study. A looped data-dependent MS/MS experimental scheme was used to acquire mass spectral data. Each cycle was composed by one full scan from m/z 450−2000 and subsequent three data-dependent product ion scans for the three most abundant ion species revealed in the full scan. To construct the 2D nano-HPLC−ESI−MS/MS system, we utilized SCX separation as the first dimensional separation. SCX chromatography is performed by 12 stepwise fractionations using elution solutions of different salt concentrations. SCX fractionated samples are subjected to RP analyses for second dimensional separation without further sample preparation. The erythrocyte protein digests were applied to the BioX-SCX column and fractionated by stepwise elution. To evaluate the performance of our system, results obtained for detection and peptide identification were compared with duplicate and nonduplicate peptide. The peptide identification for the result-

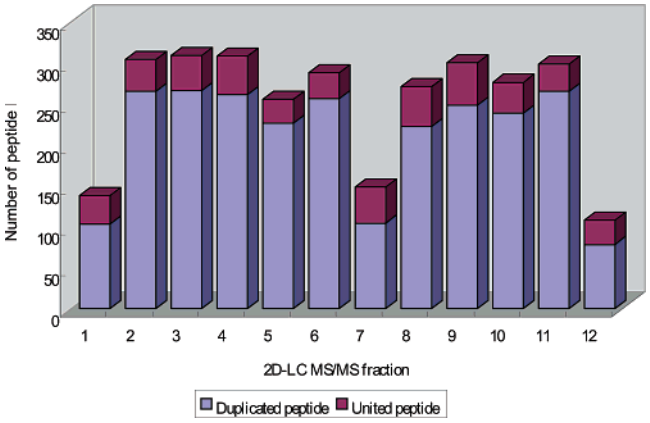

Figure 4. Number of peptide fragments identified with the inclusion criteria for MS/MS spectra.

ing MS/MS spectra was carried out using the Bioworks database search software. The SEQUEST results used to identify the protein present in the erythrocyte were filtered by applying commonly used criteria to the Xcorr and DelCn scores.[36]

The number of peptide fragments identified with the inclusion criteria for MS/MS spectra are summarized in Figure 4. Under the analytical and database search thresholds, for MS/MS score higher than the inclusion criteria on the Bioworks database search results, the ratio of duplicate peptide in 12 fractionations were from 70.3% to 88.9%, respectively (Average is 84.3%). In this experiment involving the 2D nano-HPLC−ESI−MS/MS analyses, about 3003 total peptide fragments were detected and identified, giving about 84.3% duplicate in 12 fractionations. On the other hand, about 471 nonduplicate peptide fragments were except for the pass-through fractions.

Each 2D nano-HPLC−ESI−MS/MS analysis was typically generated about 2315 MS/MS spectra. These MS/MS spectra may contain information-rich peptide fragmentation patterns and were subjected to sequence database search. A total around 27780 (2315 scans × 12 fractions) MS/MS spectra were analyzed by the database search software SEQUEST. Only a small fraction (10.8%, 3003) of searches produced significant matches according to the inclusion criteria that we used for this study. The inclusion criteria were based on Xcorr values, indices calculated by the search algorithms to reflect the similarity between product ion data and computer-simulated peptide fragmentation patterns.

These 3003 significant matches represented 362 peptides with unique short sequence stretches identified in this study. From these short sequences, the protein composition of the composite erythrocyte can be incurred. The tryptic peptides produced were often mapped to protein sequence entries in the NCBI database. The 362 unique matched peptide sequences belonged to 272 protein sequence entries in the NCBI database. Most of the 272 proteins were identified at minimal confidence level, that is, only one unique peptide sequence was matched. Positive protein identification was reported only if there were at least two product ion mass spectra of peptides matched to the sequence of a protein in the database. Among these 272 proteins, 30 proteins with at least two unique peptide sequences matched. The 30 proteins identified with higher confidence levels (at least two unique peptide sequences matched) are listed in Table 3.

The protein information and function were initially annotated by similarity searches using SWISS-Port/TrEMBL in Switzerland[44] and Bioinformatic Harvester EMBL in Germany. Apolipoprotein A-IV (apo A-IV, P01) is about growth, feeding behavior, lipid absorption and decreased cholesterol high-density lipoprotein (HDL) plasma level. It can be decreased plasma triglycerides, reduced very low-density lipoprotein (VLDL) transport rate and reduced in the plasma apolipoprotein C−III (apo C−III) level. Tropomyosin (P02, 05, 06) is the properties, kinetics and expression of these actin-associated proteins. It played important roles in regulating the length of actin filaments and thus the spectrin-actin organization and mechanical properties of the erythrocyte membrane. Cytochromes b5 (cyt b5, P03) can be defined as electron transfer proteins having one or two haem b groups, no covalently bound to the protein. Spectrin (Sp, P04, P20, P25), the most abundant of the erythrocyte membrane skeleton proteins, helps these cells maintain their characteristic biconcave shape while remaining flexible and elastic. Ran-specific GTPase-activating protein (P07) can be inhibited GTP exchange on Ran and formed a Ran-GTP-ranbp1 trimeric complex. Erythrocyte membrane protein (P08) is a multifunctional protein that mediates interactions between the erythrocyte cytoskeleton and the overlying plasma membrane. It is function to confer stability and plasticity to neuronal membrane via multiple interactions, including the spectrin-actin-based cytoskeleton, integral membrane channels and membrane-associated guanylate kinases. The myosins (P09) are a large family of motor proteins that move along actin filaments, while hydrolyzing ATP. Nef protein (P10) seems to play a role in optimizing the host cell environment for viral replication without causing cell death by apoptosis. It enhances virus infectivity and pathogenicity, also probably involved in viral immune evasion mechanisms. α-1-antitrypsin (P11) can be inhibitor of serine proteases. Its primary target is elastase, but it also has a moderate affinity for plasmin and thrombin. Albumin (P12) performs many functions including maintaining the "osmotic pressure" that causes fluid to remain within the blood stream instead of leaking out into the tissues. Apolipoprotein A-II (apo A-II, P13) may stabilize HDL structure by its association with lipids, and affect the HDL metabolism. Hemoglobin (Hb, P14, 15, 16, 26) is a protein that is carried by erythrocytes. It picks up oxygen in the lungs and delivers it to the peripheral tissues to maintain the viability of cells. Hemoglobin is made from two similar proteins that "stick together". Both proteins (α and β) must be present for the hemoglobin to pick up and release oxygen normally. The SH3 domain binding glutamic acid (P17) may be functioning as endogenous modulators of glutaredoxin 1 (GRX) activity. α-Synuclein protein (SNCA, P18) is a member of the synuclein family, which also includes β- and γ-synuclein. Synucleins are abundantly expressed in the brain and α- and β-synuclein inhibit phospholipase D2 selectively. Superoxide dismutase 1 (SOD1, P19) is a gene found in human cells that produces superoxide dismutase (SOD), an extremely potent antioxidant enzyme that fights cellular damage from reactive singlet oxygen molecules, also known as free radicals. Transthyretin (formerly prealbumin, P21) is one of 3 thyroid hormone-binding proteins found in the blood of vertebrates. It is produced in the liver and circulates in the bloodstream, where it binds retinol and thyroxine (T4). It differs from the other 2 hormone-binding proteins (T4-binding globulin and albumin) in 3 distinct ways: (1) the gene is expressed at a high rate in the brain choroid plexus; (2) it is enriched in cerebrospinal fluid; and (3) no genetically caused absence has been observed, suggesting an essential role in brain function, distinct

Table 3. 30 Erythrocyte Proteins Identified with Higher Confidence Levels (at least two unique peptide sequences matched) in This Study

serial code	NCBI accession	protein name	no. of unique peptide	peptide
P01	71797	Apolipoprotein A-IV precursor	2	-.LGEVNTYAGDLQK.- -.SELTQQLNALFQDK.-
P02	88933	Tropomyosin NM, skeletal muscle	2	-.KLVIIEGDLER.- -.MELQEIQLK.-
P03	117809	Cytochrome B5	2	-.FLEEHPGGEEVLR.- -.TFIIGELHPDDRPK.-
P04	134798	Spectrin β chain, erythrocyte (β-I spectrin)	8	-.DLAGIIAIQR.- -.EKVQLIEDR.- -.FAALEKPTTLELK.- -.KFEDFLGSMENNR.- -.LEGLDTGWDALGR.- -.LLTSQDVSYDEAR.- -.LWDELQATTK.- -.WISAMEDQLR.-
P05	136096	Tropomyosin, cytoskeletal type	2	-.EQAEAEVASLNR.- -.IQVLQQQADDAEER.-
P06	136100	Tropomyosin α chain, smooth muscle	2	-.KLVIIESDLER.- -.MEIQEIQLK.-
P07	542991	Ran-specific GTPase-activating protein	2	-.FASENDLPEWK.- -.TLEEDEEELFK.-
P08	585044	Erythrocyte membrane protein	2	-.HLIEDLIIESSK.- -.SPGIISQASAPR.-
P09	625305	Myosin heavy chain nonmuscle form A	2	-.ELEDATETADAMNR.- -.IAQLEEQLDNETK.-
P10	1401098	Nef protein	2	-.EKGGLDGLIHSK.- -.QHVARELHPEYYK.-
P11	1703025	α-1-antitrypsin precursor	5	-.DTVFALVNYIFFK.- -.GKWERPFEVK.- -.ITPNLAEFAFSLYR.- -.LSITGTYDLK.- -.SVLGQLGITK.-
P12	4502027	Albumin precursor	13	-.AFKAWAVAR.- -.AVMDDFAAFVEK.- -.DVFLGMFLYEYAR.- -.FKDLGEENFK.- -.FQNALLVR.- -.KLVAASQAALGL.- -.KQTALVELVK.- -.LKECCEKPLLEK.- -.LVAASQAALGL.- -.QTALVELVK.- -.RHPDYSVVLLLR.- -.SLHTLFGDK.- -.VPQVSTPTLVEVSR.-
P13	4502149	Apolipoprotein A-II precursor	4	-.EQLTPLIKK.- -.SKEQLTPLIK.- -.SKEQLTPLIKK.- -.VKSPELQAEAK.-
P14	4504345	Hemoglobin, α 2	5	-.FLASVSTVLTSK.- -.FLASVSTVLTSKYR.- -.LRVDPVNFK.- -.MFLSFPTTK.- -.VDPVNFK.-
P15	4504349	Hemoglobin, β	6	-.GTFATLSELHCDK.- -.LHVDPENFR.- -.SAVTALWGK.- -.VNVDEVGGEALGR.- -.VVAGVANALAHK.- -.VVAGVANALAHKYH.-
P16	4504351	Hemoglobin, δ	2	-.EFTPQMQAAYQK.- -.VNVDAVGGEALGR.-
P17	4506925	SH3 domain binding glutamic acid-rich protein like	3	-.GDYDAFFEAR.- -.QQDVLGFLEANK.- -.VYIASSSGSTAIK.-
P18	4507109	α-synuclein isoform NACP140	3	-.EGVLYVGSK.- -.EGVVHGVATVAEK.- -.TKEGVLYVGSK.-
P19	4507149	Superoxide dismutase 1	4	-.ESNGPVKVWGSIK.- -.GDGPVQGIINFEQK.- -.HVGDLGNVTADK.- -.VWGSIK.-

Table 3 (Continued)

serial code	NCBI accession	protein name	no. of unique peptide	peptide
P20	4507189	Spectrin, α, erythrocytic 1 (elliptocytosis 2)	14	-.AEDLFVEFAHK.- -.FLNVQELAAAHHEK.- -.FYLFLSK.- -.HEALENDFAVHETR.- -.HRVILENIASHEPR.- -.LEDSYHLQVFK.- -.LEDSYHLQVFKR.- -.LRGLALQR.- -.LRKHGLLESAVAAR.- -.LSESHPDATEDLQR.- -.MELNEAWEDLQGR.- -.VMALYDFQAR.- -.VQNVCAQGEDILNK.- -.YLKHQTFAHEVDGR.-
P21	4507725	Transthyretin (prealbumin, amyloidosis type I)	3	-.AADDTWEPFASGK.- -.GSpainVAVHVFR.- -.GSpainVAVHVFRK.-
P22	4557321	Apolipoprotein A−I precursor	13	-.AKVQPYLDDFQKK.- -.ATEHLSTLSEK.- -.DLATVYVDVLK.- -.DYVSQFEGSALGK.- -.KWQEEMELYR.- -.LLDNWDSVTSTFSK.- -.LSPLGEEMR.- -.QGLLPVLESFK.- -.THLAPYSDELR.- -.VKDLATVYVDVLK.- -.VQPYLDDFQK.- -.VSFLSALEEYTK.- -.WQEEMELYR.-
*P*23	4557871	Transferrin precursor	2	-.EGYYGYTGAFR.- -.MYLGYEYVTAIR.-
P24	4826762	Haptoglobin	4	-.DIAPTLTLYVGKK.- -.ILGGHLDAK.- -.TEGDGVYTLNDKK.- -.TEGDGVYTLNNEK.-
P25	5902122	Spectrin, β, nonerythrocytic 2	2	-.GEMSGRLGPLK.- -.MLTAQDVSYDEAR.-
P26	6715607	Hemoglobin, γ G	2	-.LLVVYPWTQR.- -.VNVEDAGGETLGR.-
P27	9257232	Orosomucoid 1 precursor	2	-.TYMLAFDVNDEK.- -.WFYIASAFR.-
P28	10835242	Protein kinase, cGMP-dependent, type I	2	-.AKYEAEAAFFANLK.- -.QCFQTIMMRTGLIK.-
P29	11761629	Fibrinogen, α chain,	3	-.GSESGIFTNTK.- -.MELERPGGNEITR.- -.MKPVPDLVPGNFK.-
P30	17485293	Suppression of tumorigenicity 13	2	-.LDYDEDASAMLK.- -.VAAIEALNDGELQK.-

from that played in the bloodstream it is depressed levels of serum retinol, retinol binding protein, and thyroid hormone. Apolipoprotein A−I (apoA-I, P22) participates in the reverse transport of cholesterol from tissues to the liver for excretion by promoting cholesterol efflux from tissues and by acting as a cofactor for the lecithin cholesterol acyltransferase (lcat). Transferrin (*P*23) is a plasma protein that transports iron through the blood to the liver, spleen, and bone marrow. The blood transferrin level is tested for diverse reasons: to determine the cause of anemia, to examine iron metabolism (for example, in iron deficiency anemia) and to determine the iron-carrying capacity of the blood. Haptoglobin (P24) combines with free plasma hemoglobin, preventing loss of iron through the kidneys and protecting the kidneys from damage by hemoglobin, while making the hemoglobin accessible to degradative enzymes. Orosomucoid 1 (ORM1, P27) appears to function in modulating the activity of the immune system during the acute-phase reaction. Protein kinase, cGMP-dependent, type I (P28) is interacting selectively with 3′,5′-cGMP, the nucleotide guanosine 3′,5′-cyclophosphate and interacting selectively with ATP, adenosine 5′-triphosphate, a universally important coenzyme and enzyme regulator. Fibrinogen (factor I, P29) is synthesized by liver. Fibrinogen is converted to fibrin, in the formation of a blood clot, via the enzymatic action of thrombin. A lack of fibrinogen may be congenital or acquired. A condition known as disseminated intravascular coagulation (DIC) results in the excessive utilization and depletion of fibrinogen. Suppression of tumorigenicity 13 (P30) has antiproliferative properties in human melanoma cells and may contribute to terminal cell differentiation. It may also function as a negative regulator of melanoma progression

Figure 5 showed the distribution of cellular locations of proteins identified in this study. Among 272 proteins identified, 79 proteins (29%) were known to be secreted into extracellular space. Forty-seven proteins (17%) were known to be membrane and cytoskeleton protein. Thirty proteins (11%) were known to be cytoplasma proteins. Twenty-eight proteins (10%) were known to be nuclear proteins. Seven proteins (3%) were

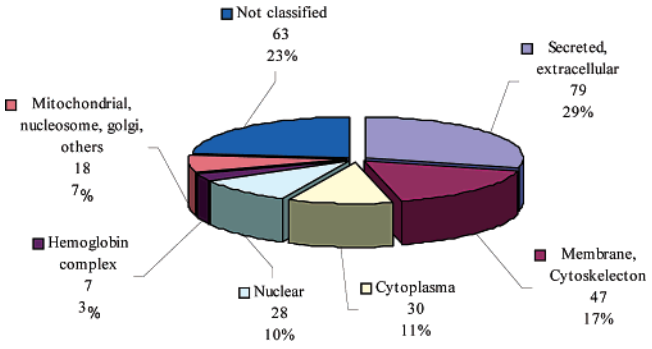

Figure 5. Distribution of cellular locations of 272 proteins identified in this study.

hemoglobin complex. A few mitochondrial, nucleosome and golgi proteins were also identified. A considerable portion of the identified proteins (23%, 63 proteins) has not been reported for their cellular locations.

We used the ExPASy (Expert Protein Analysis System) proteomics server of the Swiss Institute of Bioinformatics (SIB) to explore what known functions of the identified proteins had been reported in the literature. Swiss-Prot/TrEMBL[44] was used to obtain relevant information regarding to the functions of the 272 proteins. Figure 6 shows the number and percentage of proteins with certain reported known biological process and molecular functions. Among 272 proteins, 62 proteins were binding proteins. Fifty-seven proteins were about metabolism. Forty-three proteins have been known to be associated with cell growth and/or maintenance, and forty-one proteins have been known to be associated with catalytic activity. Protein functions related to structure molecule activity, immune response, defense/immunity protein activity and cell communication were also surveyed, and these functions were linked to considerable portions of 272 proteins identified in this study. Some proteins still had no prior functional information reported.

Conclusion

The results presented provide an example of the 11-mercaptoundecanoic acid SAMs applications for the enzyme digestion chip and established 2D nano-HPLC−ESI−MS/MS analysis of proteins. It is a powerful method capable of displaying the protein identification in an organ without the requirement of detailed knowledge of individual proteins. The technology available for studying proteome expression and resolving exact protein and peptide identities in complex mixtures of biological samples allows global protein expression within cells, fluids, and tissue to be approached with confidence.

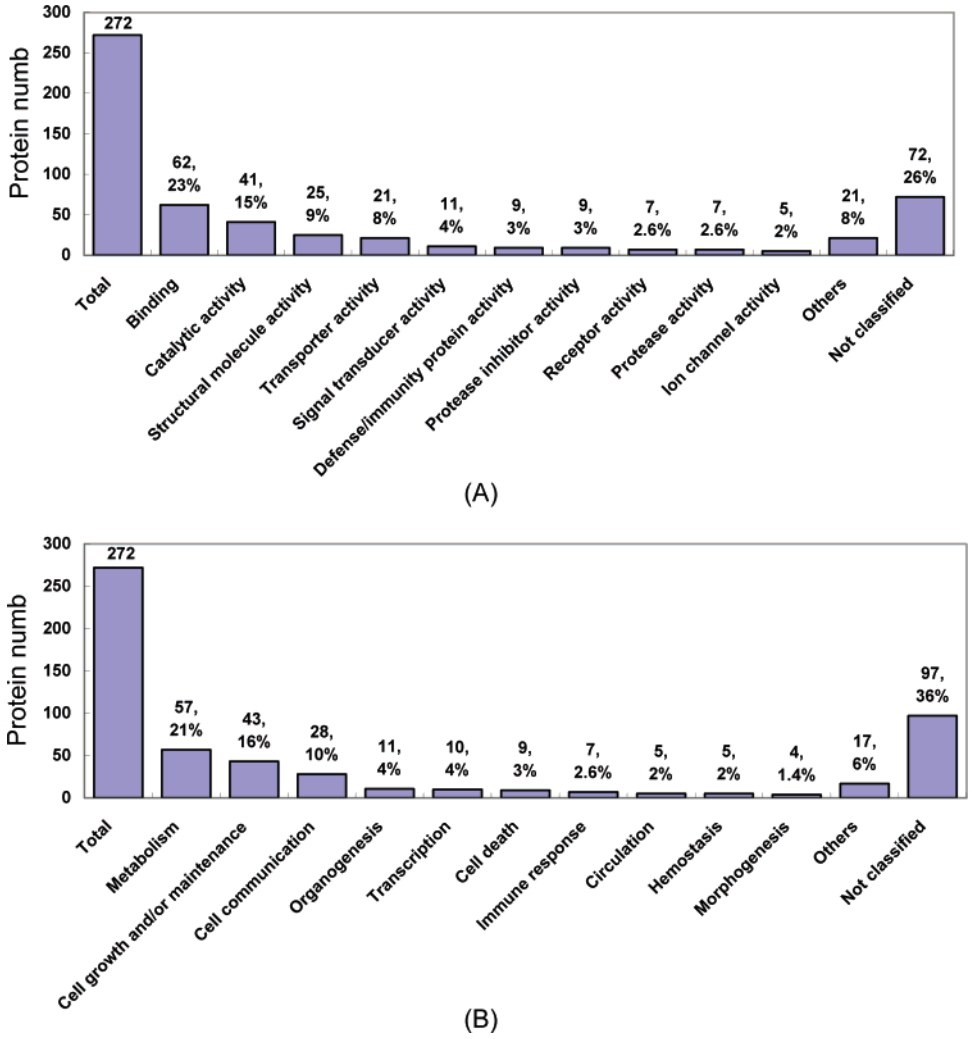

Figure 6. Number and percentage of proteins with certain reported known biological process (A) and molecular functions (B).

SAMs formation provides an easy way to prepare the structure that can be further functionalized with biomolecules to yield biorecognition surfaces for use in medical devices. The application of SAMs for the immobilization of enzymes to Au surfaces has considerable potential to produce reproducible enzyme biochips. In summary, we have presented the modification of Au interface via 11-mercaptoundecanoic acid SAMs and proved that the SAMs on Au can be a trypsin digestion chip for proteins analysis by 2D nano-HPLC−ESI−MS/MS. The data form a database for the diversity and relative abundance of various proteins found in the erythrocyte proteins. In the current proteomic study, we have assembled an enlarged list of proteins observed in erythrocyte by combining the proteomics approaches.

Acknowledgment. The authors thank National Cheng-Kung University Proteomics Research Core Laboratory for the assistance in protein identification. This work was partially supported by grants (NSC92-2113-M006-022) from the National Science Council.

References

(1) Tyers, M.; Mann, M. *Nature* **2003**, *422*, 193−197.
(2) Fujii, K.; Nakano, T.; Kawamura, T.; Usui, F.; Bando, Y.; Wang, R.; Nishimura, T. *J. Proteome Res.* **2004**, *3*, 712−718.
(3) Hamler, R. L.; Zhu, K.; Buchanan, N. S.; Kreunin, P.; Kachmam, M. T.; Miller, F. R.; Lubman, D. M. *Proteomics* **2004**, *4*, 562−577.
(4) Wolters, D. A.; Washburn, M. P.; Yates, J. R. *Anal. Chem.* **2001**, *73*, 5683−5690.
(5) Horne, J. C.; Blanchard, G. J. *J. Am. Chem. Soc.* 1**998**, *120*, 6336−6344.
(6) Morhard, F.; Schumacher, J.; Lenenbach, A.; Wilhelm, T.; Dahint, R.; Grunze, M.; Everhart, D. S. *Proc.-Electrochem. Soc.* **1997**, *19*, 1058−1065.
(7) Bierbaum, K.; Grunze, M.; Baski, A. A.; Chi, L. F.; Schrepp, W.; Fuchs, H. *Langmuir* **1995**, *11*, 2143-2150.
(8) Schertel, A.; Woll, C.; Grunze, M. *J. Phys.* **1997**, *7*, 537−538.
(9) Yan, C.; Zharnikov, M.; Goelzhaeuser, A.; Grunze, M. *Langmuir* **2000**, *16*, 6208−6215.
(10) Himmel, H. J.; Weiss, K.; Jaeger, B.; Dannenberger, O.; Grunze, M.; Woell, C. *Langmuir* **1997**, *13*, 4943−4947.
(11) Jung, C.; Dannenberger, O.; Xu, Y.; Buck, M.; Grunze, M. *Langmuir* **1998**, *14*, 1103−1107.
(12) Bain, C. D.; Troughton, E. B.; Tao, Y.; Evall, J.; Whitesides, G. M.; Nuzzo, R. G. *J. Am. Chem. Soc.* **1989**, *111*, 321−335.
(13) Ulman, A. *An Introduction to Ultrathin Origanic Films*; Academic Press: San Diego, 1991.
(14) Dubois, L. H.; Nuzzo, R. G. *Annu. Rev. Phy. Chem.* **1992**, *43*, 437−463.
(15) Ulman, A. *Chem. Rev.* **1996**, *96*, 1533−1554.
(16) Laibinis, P. E.; Nuzzo, R. G. *J. Phys. Chem.* **1992**, *96*, 5097−5105.
(17) Joyce, S. A.; Thomas, R. C.; Houston, J. E.; Michalske, T. A.; Crooks, R. M. *Phys. Rev. Lett.* **1992**, *68*, 2790−2793.
(18) Gooding, J. J.; Hibbert, D. B. *Trends Anal. Chem.* **1999**, *18*, 525−533.
(19) Erdelen, C.; Häussling, L.; Naumann, R.; Ringsdorf, H.; Wolf, H.; Yang, J.; Liley, M.; Spinke, J.; Knoll, W. *Langmuir* **1994**, *10*, 1246−1250.
(20) Laibinis, P. E.; Whitesides, G. M. *J. Am. Chem. Soc.* **1992**, *114*, 9022−9028.
(21) Buerk, D. G. *Biosensor: Theory and Applications*; Technol. Pub. Comput. Inc.: New York, 1993.
(22) Kang, I. K.; Kwon, B. K.; Lee, J. H.; Lee, H. B. *Biomaterials* **1993**, *14*, 792−797.
(23) Tyan, Y. C.; Liao, J. D.; Kalause, R.; Wu, I. D.; Weng, C. C. *Biomaterials* **2002**, *23*, 65−76.
(24) Frey, B. L.; Corn, R. M. *Anal. Chem.* **1996**, *68*, 3187−3193.
(25) Smith, E. L.; Alves, C. A.; Andereg, J. W.; Porter, M. D.; Siperko, L. M. *Langmuir* **1992**, *8*, 2707−2714.
(26) Sun, L.; Crooks, R. M.; Ricco, A. J. *Langmuir* **1993**, *9*, 1775−1780.
(27) Miura, Y.; Kimura, S.; Imanishi, Y.; Umemura, J. *Langmuir* **1999**, *15*, 1155−1160.
(28) Delden, C. J.; Lens, J. P.; Kooyman, R. P. H.; Engbers, G. H. M.; Feijen, J. *Biomaterials* **1997**, *18*, 845−852.
(29) Kuijpers, A. J.; Wachem, P. B.; Luyn, M. J. A.; Brouwer, L. A.; Engbers, G. H. M.; Krijgsveld, J.; Zaat, S. A. J.; Dankert, J.; Feijen, J. *Biomaterials* **2000**, *21*, 1763−1772.
(30) Yang, J. M.; Wang, M. C.; Hsu, Y. G.; Chang, V. H.; Lo, S. K. *J. Appl. Polym. Sci.* **1998**, *138*, 19−27.
(31) Yang, J. M.; Jong, Y. J.; Hsu, K. Y.; Chang, C. H. *J. Biomed. Mater. Res.* **1998**, *39*, 86−91.
(32) Lestelius, M.; Liedberg, B.; Tengvall, P. *Langmuir* **1997**, *13*, 5900−5908.
(33) Marcus, K.; Immler, D.; Sternberger, J.; Meyer, H. E. *Electrophoresis* **2000**, *21*, 2622−2636.
(34) Bradford, M. M. *Anal. Biochem.* **1976**, *72*, 248−254.
(35) Schwartz, H.; Mitulovic, G.; Soest, R. V.; Gils, M. V.; VerBerkmoes, N.; Hettich, R. *PharmaGenomics* **2002**, *July*, 42−50.
(36) Wolters, D. A.; Washburn, M. P.; Yate, III, J. R. *Anal. Chem.* **2001**, *73*, 5683−5690.
(37) Noble-Luginbuhl, A. R.; Nuzzo, R. G. *Langmuir* **2001**, *17*, 3937−3944.
(38) Chidsey, C. E. D.; Loiacono, D. N. *Langmuir* **1990**, *6*, 682−691.
(39) Laibinis, P. E.; Whitesides, G. M.; Allara, D. L.; Tao, Y. T.; Parikh, A. N.; Nuzzo, R. G. *J. Am. Chem. Soc.* **1991**, *113*, 7152−7167.
(40) Ito, Y.; Kajihara, M.; Imanishi, Y. *J. Biomed. Mater. Res.* **1991**, *25*, 1325−1337.
(41) Tyan, Y. C.; Liao, J. D.; Lin, S. P.; Chen, C. C. *J. Biomed. Mater. Res.* **2002**, *67A*, 1033−1043.
(42) Moulder, J. F.; Stickle, W. F.; Sobol, P. E.; Bomben, K. D. *Handbook of X-ray Photoelectron Spectroscopy*; Physical Electronics, Inc.: Eden Prairie, Minnesota, 1995; 42−43.
(43) Beamson, G.; Briggs, D. *High-Resolution XPS of Organic Polymers. The Scienta ESCA300 Database*; Wiley & Sons Inc.: New York, 1992.
(44) O'Donovan, C.; Martin, M. J.; Gattiker, A.; Gasteiger, E.; Bairoch, A.; Apweiler, R. *Brief. Bioinform.* **2002**, *3*, 275−284.

PR0497780